Department of Physics and Astronomy
University of Heidelberg

Fourier transformation on the sphere

Bachelor Thesis in Physics
submitted by

Philipp Herz

born in Schwäbisch Hall (Germany)

August 2020

under the supervision of Prof. Dr. Björn Malte Schäfer

Contents

Abstract

Fourier transforms for fields on the sphere are a common problem in astrophysics and cosmology. Those fields can be represented by spherical harmonics, which we wanna relate to the Fourier transform. Analyzing the geometric aspects of the Archimedean spiral for a high number of turns $N \gg 1$, such as the behaviour of unit vectors of a tangent plane along the spiral on the surface compared to unit vectors $\vec{e}_\theta$ and $\vec{e}_\varphi$ of the sphere: Along the spiral from one pole to the equator the tangent vector $\vec{t}$ converges towards the unit vector $\vec{e}_\varphi$ and diverges from the unit vector $\vec{e}_\theta$. The Archimedean spiral can be projected via the Euler spiral on a flat one dimensional Euclidean space, on which Fourier Transformations are quickly carried out by so called Fast Fourier transformations, it is also possible to carry out the Fourier transformations in the tangent plane along the Archimedean spiral on the surface of the sphere. For the pixelisation we proposed to use the Igloo pixelisation, which allows pixels to be arranged along the spiral with a constant latitude.

Further we analyzed differential geometric aspects such as the generated metric, the Riemann tensor, by using that we are operating on a maximally symmetric manifold, the Ricci tensor and Ricci scalar, which remains the value of 2. In addition we asked the question: Is the Archimedean spiral a geodesic? Indeed, for a high number of turns at the equator.

By changing the (θ, φ)-basis to a tangent plane basis (u, v) in the Edth operator $\eth$, we were able to give an idea how to construct eigenfunctions $\tilde{Y}_{\ell m}$ of the Laplace equation and relate the one dimensional Fourier transform along the spiral with a two dimensional decomposition of a field on the sphere in spherical harmonics.

1 Introduction

The idea behind this thesis is to map data points on the surface of a sphere onto a flat plane. This is a bijective mapping which projects points in a distorting way, we want to minimize the distortion. As example the stereographic projection has an awfully high distortion in its projection of the Earth (as a globe) as seen below. Because the distortion is unacceptable we would like to come up with another mapping option:
We compare an Archimedean spiral on the surface of a sphere with a spiral on a flat, Euclidean surface, due to the behaviour of the spiral we get an Euler-spiral in 2D. If we now increase the number of turns of the spiral on the sphere, the curvature of the Euler spiral gets closer to 0.

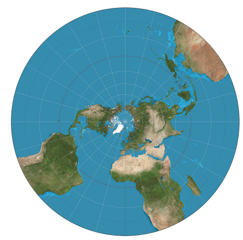

Figure 1: Stereographic projection of the earth

1.1 Map making on a sphere

1.1.1 Archimedean spiral

The Archimedian spiral is a spherical spiral on the surface of a sphere, the latitude angle θ runs from 0 to π while the azimuthal angle φ is linear proportional to the θ-angle with the relation:

$$\varphi = 2N \cdot \theta$$

with N being the number of turns around the sphere (Figure 2 shows a spherical spiral with $N = 10$ turns.). For further derivations we can write the parametrisation in two ways, equation (1.1) shows the description in the (θ, φ)-basis , while equation (1.2) describes the curve in the Cartesian coordinate system.

$$\vec{\gamma} = (\theta, 2N\theta)^{\perp}_{\theta,\varphi} \tag{1.1}$$

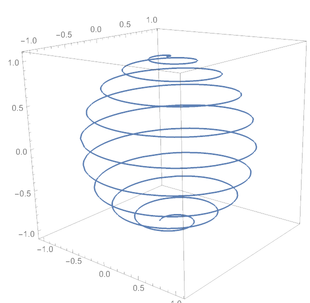

Figure 2: Spherical spiral at $N = 10$

The curve is parametrized as:

$$\vec{\gamma} = \begin{bmatrix} \sin(\theta)\cos(2N\theta) \\ \sin(\theta)\sin(2N\theta) \\ \cos(\theta) \end{bmatrix} \tag{1.2}$$

1.1.2 Euler spiral

The Euler spiral is parametrized through the following two integrals, with B being the arc length of the spiral and N the number of turns:

$$\begin{aligned} x(B) &= \int_0^B \mathrm{d}u \cos \sqrt{(2\pi N)^2 - u^2} \\ y(B) &= -\int_0^B \mathrm{d}u \sin \sqrt{(2\pi N)^2 - u^2} \end{aligned} \tag{1.3}$$

which can be expressed in imaginary units $z = x + \mathrm{i}y$, with $x, y \in \mathbb{R}$:

$$z(t) = \int_0^B \exp\left(\mathrm{i}\sqrt{(2\pi N)^2 - u^2}\right) \mathrm{d}u \tag{1.4}$$

Therefore is every point on the Archimedean spiral (three dimensions) represented through one point on the Euler spiral (two dimensions), which is given through the arc length B.

1.2 Curvature and curves on a sphere

If you take a look at a curve, there are mainly two properties which are interesting: The length and the curvature (While in this context the curvature is a property of the manifold the curve is projected on). Because the length depends on the curvature it is important to discuss how one can qualitatively examine the curvature. A straight line increases its length from a flat surface spanned over a convex/concave surface. So what is a manifold and how is this curvature determined?

1.2.1 Manifold

Locally an n-dimensional manifold M is nothing else than an Euclidean space $\mathbb{R}^n$, which helps us to work with our spiral. We use so small (θ, φ)-angles that we can make the approximation that the curvature of the sphere is vanishing locally. Globally a manifold does not need to be homeomorphic to Euclidean space, which is the case for the surface of a sphere. The sphere is a two-dimensional manifold, and the vanishing curvature is best visible in an atlas of the Earth, locally the distances in a chart are quite correct, but if you would map the entire globe onto one flat surface and look at global distances, so that the metric approximation through the Euclidean one is not appropriate, you would be able to find different distances. The curvature determines the size of the region in which the Euclidean metric approximation is appropriate. Nevertheless we are working in this thesis with Riemann manifolds, which require a Riemann metric, the metric tensor $g_{\mu\nu}$, which profess a structure of the manifold. This metric tensor defines the scalar product $\mathrm{d}s^2 = g_{\mu\nu}\mathrm{d}x^\mu\mathrm{d}x^\nu$ in the tangent space T_pM at every point p on the manifold M. This scalar product defines us distances of vectors and angles between them. Equipped with this metric tensor we can derive lengths of curves and lengths between points on the manifold.

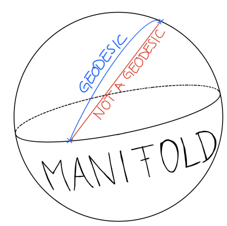

Figure 3: Visualization of a straight line (geodesic) on a manifold

1.2.2 Metric

Now we know what a manifold is and how we can compute distances on it. The Riemann curvature tensor is derived from the metric tensor $g_{\mu\nu}$. In the following the Einstein summation convention is used. The metric tensor can be transformed by Jacobi-matrices. With the embedding map $f : M \to N$, with components f^α, we can calculate the metric tensor on the submanifold M of an n-dimensional Riemann manifold N:

$$g_{M\,\mu\nu}(x)\mathrm{d}x^\mu \mathrm{d}x^\nu = g_{N\,\alpha\beta}(f(x))\frac{\partial f^\alpha}{\partial x^\mu}\frac{\partial f^\beta}{\partial x^\nu}\mathrm{d}x^\mu \mathrm{d}x^\nu \tag{1.5}$$

1.2.3 Levi-Civita connection and Christoffel-symbols

For a given coordinate system x^i with $i = 1, 2, ..., n$ on an n-dimensional manifold M, we can express the tangent vectors which can be labeled as local tangent basis as:

$$\vec{e}_i = \frac{\partial}{\partial x^i} = \partial_i \tag{1.6}$$

If we now wanna know the change of those tangent basis' this can be expressed by the Christoffel symbols:

$$\Gamma^k{}_{ij} = \frac{\partial \vec{e}_i}{\partial x^j} \cdot \vec{e}^{\,k} \tag{1.7}$$

However, this expression holds in Euclidean space. For a Riemann manifold this change of a tangent basis is given through derivatives of the metric $g_{\mu\nu}$:

$$\Gamma^k_{ij} = \frac{1}{2}g^{kl}\Big(\partial_i g_{jl} + \partial_j g_{il} - \partial_l g_{ij}\Big) \tag{1.8}$$

We are operating on tangent spaces of Riemann manifolds: T_pM. The properties of those tangent spaces depend on the point p they are spanned from. A manifold has a lot of different tangent spaces, those can be summed up to a tangent bundle, we are now searching for a connection on this tangent bundle, i.e. a connection from tangent space T_pM at position p to tangent space T_qM at position q. The metric $g_{\mu\nu}$ describes the geometry of our manifold, so it is clear that the (Levi-Civita) connection should preserve the metric, which can be written like this

$$\nabla_\alpha g^{\mu\nu} = 0 \tag{1.9}$$

The second condition for the connection is the torsion-freeness, which is in our case the symmetry of the Christoffel symbols in the two lower indices:

$$\Gamma^k_{ij} = \Gamma^k_{ji} \tag{1.10}$$

∇ is the connection on the Riemann manifold. The Levi-Civita connection can than be expressed as

$$\nabla_{\partial_i}\partial_j = \Gamma^k_{ij}\partial_k \tag{1.11}$$

For ∂_i being a coordinate basis.

1.2.4 Geodesic equation

Now we want to have a look at straight lines. On a flat manifold (curvature is zero) a straight line would be drawn with a ruler, but the same ruler would not be able to draw a straight line on a curved manifold. A straight line on a curved manifold is called a geodesic and connects two points with the shortest path between them. A curve x^μ can be determined as geodesic if the following geodesic equation holds:

$$\frac{\partial^2 x^\mu}{\partial \tau^2} + \Gamma^\mu_{\alpha\beta} \frac{\partial x^\alpha}{\partial \tau} \frac{\partial x^\beta}{\partial \tau} = 0 \tag{1.12}$$

while τ is an affine parameter along the curve, i.e. proper time. The geodesic equation can be derived from the equivalence principle or the variation of an action using Hamilton's principle. Further, all geodesics on the S^2 are great circles, a proof can be found here: [4].

1.2.5 Riemann curvature tensor

With the Christoffel symbols we can now compute the Riemann curvature tensor $R^\rho{}_{\sigma\mu\nu}$.

$$R^\rho{}_{\sigma\mu\nu} = \partial_\mu \Gamma^\rho{}_{\nu\sigma} - \partial_\nu \Gamma^\rho{}_{\mu\sigma} + \Gamma^\rho{}_{\mu\lambda} \Gamma^\lambda{}_{\nu\sigma} - \Gamma^\rho{}_{\nu\lambda} \Gamma^\lambda{}_{\mu\sigma} \tag{1.13}$$

If the Riemann tensor is vanishing than the Riemann manifold is flat, which is the case for small angles (locally), more about it in chapter 3. Further one can derive the Ricci tensor $R_{\mu\nu}$ and the Ricci-scalar R, which is the trace of the Ricci tensor.

$$R_{\mu\nu} = g^{\gamma\delta} R_{\gamma\mu\delta\nu} = g_{\gamma\rho} R^\rho{}_{\mu\delta\nu} \tag{1.14}$$

$$R = g^{\mu\nu} R_{\mu\nu} \tag{1.15}$$

For our derivation we use that a sphere is a maximally symmetric manifold of dimension 2, which connects the Riemann tensor directly with the metric tensor $g_{\mu\nu}$:

$$R_{abcd} = \frac{R}{2} \Big(g_{ac} g_{db} - g_{ad} g_{cb} \Big) \tag{1.16}$$

With R being the Ricci tensor. An idea of the derivation of (1.16) is given in chapter 3.

1.3 Pixelisation

1.3.1 HEALPix

Hierarchical **E**qual **A**rea iso**L**atitude **P**ixelisation is an method to discretize the surface of the sphere such that spherical harmonic transforms can be carried out efficiently. The surface of the sphere is divided into twelve basis pixels, of which every pixel can be divided by four other pixels, of which every pixel can be divided into four pixels again in a recursive way. The pixels of HEALPix method have three main properties:

- As mentioned, the pixels can be divided, which is a playful tool for resolution.
- The pixels have the same size.
- The pixels are arranged on circles of constant latitudes

The last point is essential for the efficient calculation of the spherical harmonics. The spherical harmonics enable us to decompose a wave into the composition of different wave-lengths. At constant latitude we are left with a Fourier-transform, which is easy to carry out:

$$a(\theta) = \sum_{\ell} \sum_{m=-\ell}^{\ell} a_{\ell m} Y_{\ell m}(\theta, \varphi) \tag{1.17}$$

$$Y_{\ell m}(\theta, \varphi) = \sqrt{\frac{2\ell + 1}{4\pi}} \sqrt{\frac{(\ell - |m|)!}{(\ell + |m|)!}} P_{\ell m}(\cos(\theta)) e^{\mathrm{i}m\varphi} \tag{1.18}$$

$$\rightarrow a_{\ell m} = \int \mathrm{d}\Omega \; a(\theta, \varphi) Y^*_{\ell m}(\theta, \varphi) \tag{1.19}$$

In which the to examined field is $a(\theta, \varphi)$ and the decomposition coefficients are $a_{\ell m}$.

1.3.2 Spiral pixelisation

The most natural way to discretize the surface, of for instance the cosmological background radiation, would be pixels which are arranged along the spiral. This means that the resolution of the data would control the number of turns N of the spiral. The pixel size depends on the distance between two points beneath each other on the spiral. The distance between two points can be approximated by

$$\Delta\vec{\gamma} = \vec{\gamma}_0 - \vec{\gamma}_1 \tag{1.20}$$

which delivers us the vertical distance between two points. If we now choose a $\theta = \theta_0$ we can calculate the φ-angle, which is $\varphi_0 = 2N\theta_0$. Now we want to make one loop around the surface of the sphere:

$$\varphi_1 = \varphi_0 + 2\pi = 2N\theta_0 + 2\pi \tag{1.21}$$

From here we can calculate the corresponding θ_1-angle:

$$\theta_1 = \frac{\varphi_1}{2N} = \frac{2N\theta_0 + 2\pi}{2N} = \theta_0 + \frac{\pi}{N} \tag{1.22}$$

Which seems to be right, because for increasing number of turns the distance between two points on the spiral beneath each other should be converging to zero. For small angles we can approximate $\sin\alpha \approx \alpha$, therefore the distance between two points reduces to:

$$|\Delta\gamma^{\theta}| \approx |\theta_1 - \theta_0| = \frac{\pi}{N} \tag{1.23}$$

It also makes sense that it does not depend on the position of the points because the distance between the lines is always constant. The second length of the pixel is determined through the difference of two neighbouring φ-angles. This width of a pixel is a property of the resolution of the displayed data. In general the Igloo pixelisation [2] is an appropriate candidate, for which we calculated the height of all pixels. In Figure 4

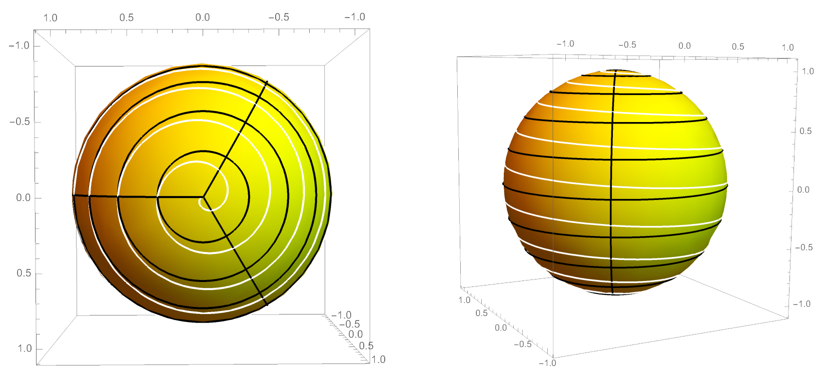

(a) Spiral with $N = 10$ turns from above (b) Spiral with $N = 10$ turns parallel to z-axis

Figure 4: Igloo pixelisation with θ-spacing of π/N

the Igloo pixelisation pattern is for $N = 10$ plotted. One can see that the Archimedean spiral does not cross a single pixel two times, which is important to eliminate the problem of periodicity, which would not be given in the data.

1.4 Fourier transformation and spherical harmonics

Fourier transformation is a method which decomposes a signal into a spectrum (of which both can be periodic and continuous). For a (integrable) function $f \in L^1(\mathbb{R}^n)$ the Fourier transformation $\hat{f}$ of f is given through the integral

$$\hat{f}(\vec{l}) = \frac{1}{(2\pi)^{n/2}} \int_{\mathbb{R}^n} f(\vec{\theta}) e^{-\mathrm{i}\vec{l}\cdot\vec{\theta}} \mathrm{d}\vec{\theta} \tag{1.24}$$

and the inverse transformation is given through:

$$f(\vec{\theta}) = \frac{1}{(2\pi)^{n/2}} \int_{\mathbb{R}^n} \hat{f}(\vec{l}) e^{\mathrm{i}\vec{l}\cdot\vec{\theta}} \mathrm{d}\vec{l} \tag{1.25}$$

With $\vec{\theta}$ being a vector in the tangent plane spanned by local coordinates θ_x and θ_y. These plane waves are the eigenfunctions of the Laplace equation in cartesian coordinates:

$$\Delta f(\vec{x}) = -k^2 f(\vec{x}) \text{ with } f(\vec{x}) = e^{i\vec{k}\vec{x}} \tag{1.26}$$

The same expression in spherical coordinates leads to different eigenvalues and eigenfunctions, equation (1.18).

$$\Delta_{\theta,\varphi} Y_{\ell m}(\theta,\varphi) = -\ell(\ell+1) Y_{\ell m}(\theta,\varphi) \tag{1.27}$$

Observing the limit for $\ell \gg 1$ of equation (1.27) leads to equation (1.26). The meaning of this is to reduce the observed arc length on the surface of the sphere and approximate the neighbourhood around a point on the surface through a plane. Further the spherical harmonics (1.18) form a complete set of orthonormal functions:

- Orthonormal relation (δ_{ij} is the Kronecker delta)

$$\int_{S^2} Y^*_{\ell' m'}(\theta,\phi) Y_{\ell m}(\theta,\phi)\, \mathrm{d}\Omega = \delta_{\ell' m'}\, \delta_{\ell m} \tag{1.28}$$

  While the upper star $Y^*_{\ell m}$ denotes the complex conjugate to $Y_{\ell m}$.

- the completeness relation ($\delta_D(x)$ is the δ-distribution)

$$\sum_{\ell=0}^{\infty} \sum_{m=-\ell}^{\ell} Y^*_{\ell m}(\theta', \phi') Y_{\ell m}(\theta,\phi) = \delta_D(\theta' - \theta)\, \delta_D(\varphi' - \varphi) \tag{1.29}$$

In words: The first property tells us that the spherical harmonics are an orthonormal system, every $Y_{\ell m}$ is perpendicular to $Y_{\ell' m'}$, if $\ell \neq \ell'$ or $m \neq m'$. The second property tells us that the spherical harmonics build a complete set, which means that every real valued spherical function f can be described as a linear combination of spherical harmonics, as described in equation (1.17) and (1.19). Which can also be accounted for the Fourier transformation, every periodic function can be decomposed into plane waves and the plane waves build a complete set:

$$\int e^{i\vec{k}\vec{x}} e^{-i\vec{k'}\vec{x}} \mathrm{d}\vec{x} = \int e^{-i(\vec{k'}-\vec{k})\vec{x}} \mathrm{d}\vec{x} = \delta_D(\vec{k'} - \vec{k}) \tag{1.30}$$

These Fourier transforms can be carried out quite fast with **F**ast **F**ourier **T**ransforms (FFT) [1], especially when the number of data points decomposes in many small prime factors.[3] For a function $a(\theta, \varphi)$ which is decomposed into spherical harmonics $Y_{\ell m}$ and for a constant latitude θ_0, the coefficients $a_{\ell m}$ (equation 1.19) can be carried out quite easily because the φ part in $\mathrm{d}\Omega$ correspond to a Fourier transformation.

1.5 Edth operator $\eth$

It is possible to adapt the spherical harmonics $Y_{\ell m}$ to spin-weighted spherical harmonics ${}_sY_{\ell m}$. These spin weighted spherical harmonics are still functions on the sphere but have one more parameter s which is referred to as spin weight. Functions with spin weight are defined by a rotation around the north pole:

$$ {}_sf(\vec{m}', \vec{n}) = e^{\mathrm{i}s\gamma}\, {}_sf(\vec{m}, \vec{n}) \text{ with } \vec{m}' = e^{\mathrm{i}\gamma}\vec{m} \tag{1.31} $$

while $\vec{m} \in \mathbb{C}^n$. By defining an operator $\eth$ we can raise or lower the spin weight of a function ${}_sf$ to ${}_{s+1}f$ or ${}_{s-1}f$.

$$ \begin{aligned} \eth\, {}_sf &= -(\sin\theta)^s[\partial_\theta + \mathrm{i}\csc\theta\partial_\varphi](\sin\theta)^{-s}\, {}_sf \\ \bar{\eth}\, {}_sf &= -(\sin\theta)^s[\partial_\theta - \mathrm{i}\csc\theta\partial_\varphi](\sin\theta)^{-s}\, {}_sf \end{aligned} \tag{1.32} $$

With this operator the spin weighted spherical harmonics are defined as

$$ \begin{aligned} {}_sY_{\ell m} &= \sqrt{\frac{(\ell - s)!}{(\ell + s)!}}\, \eth^s\, Y_{\ell m} && \text{for } 0 \leq s \leq \ell \\ {}_sY_{\ell m} &= \sqrt{\frac{(\ell + s)!}{(\ell - s)!}}\, \bar{\eth}^{-s} Y_{\ell m} && \text{for } -\ell \leq s \leq 0 \\ {}_sY_{\ell m} &= 0 && \text{for } \ell < |s| \end{aligned} \tag{1.33} $$

which leads for a spin weight of $s = 0$ to the spherical harmonics ${}_0Y_{\ell m} = Y_{\ell m}$. This representation of the spin weighted spherical harmonics leads to shifting property of the edth operator:

$$ \begin{aligned} \eth({}_sY_{\ell m}) &= +\sqrt{(\ell - s)(\ell + s + 1)}\, {}_{s+1}Y_{\ell m} \\ \bar{\eth}({}_sY_{\ell m}) &= -\sqrt{(\ell + s)(\ell - s + 1)}\, {}_{s-1}Y_{\ell m} \end{aligned} \tag{1.34} $$

2 Archimedean Spiral

Using the information given in the Introduction we want now to examine the Archimedean spiral a bit more.

2.1 Arc length

First, we want to describe the spiral through the arc length, so we have a variable parameter which describes each point on the spiral bijectively. This would make the mapping much easier.

2.1.1 Derivation of the arc length

The arc length is calculated by the sum of the derivatives respect to the θ-angle. We keep in mind that $\theta \in [0, \pi]$.

$$\begin{aligned}
B &= \int_a^b \mathrm{d}\theta \sqrt{\dot{x}^2 + \dot{y}^2 + \dot{z}^2} \\
&= \int_0^\theta \mathrm{d}\theta' \sqrt{1 + 4N^2 \sin^2\theta'} \\
&\cong \int_0^\theta \mathrm{d}\theta' \Big[(\sqrt{1+4N^2} - 1) \sin\theta' + 1 \Big] \quad \text{for the approximation: referring to Appendix A.1} \\
&= \Big(\sqrt{1+4N^2} - 1 \Big) \Big[-\cos\theta' \Big]_0^\theta + \theta \\
&= \Big(\sqrt{1+4N^2} - 1 \Big) \Big(1 - \cos\theta \Big) + \theta \qquad 1 \ll N \text{ and dropping } \theta : \theta \ll N \\
&\cong \sqrt{1+4N^2} \Big(1 - \cos\theta \Big)
\end{aligned} \tag{2.1}$$

Bringing this into a nicer form and answering the question at which latitude I am for a given arc length and number of turns.

$$\cos(\theta) = 1 - \frac{B}{\sqrt{1+4N^2}} \tag{2.2}$$

$$\Rightarrow B \in [0, 2\sqrt{1+4N^2}]$$

Therefore we can now calculate the upper bound of the arc length, it is a natural cause that it depends on the number of turns.

Using this information we just derived, we can now express the curve $\vec{\gamma}$ through the arc length and the number of turns.

$$\vec{\gamma} = \begin{bmatrix} \sqrt{\frac{2B}{\sqrt{1+4N^2}} - \frac{B^2}{1+4N^2}} \cos(2N \arccos(1 - \frac{B}{\sqrt{1+4N^2}})) \\ \sqrt{\frac{2B}{\sqrt{1+4N^2}} - \frac{B^2}{1+4N^2}} \sin(2N \arccos(1 - \frac{B}{\sqrt{1+4N^2}})) \\ 1 - \frac{B}{\sqrt{1+4N^2}} \end{bmatrix} \tag{2.3}$$

2.1.2 Pixelisation of the Sphere

We expressed the spiral through its arc length, the easiest way to pixelate the surface of the sphere would be pixels along the spiral. But this raises the question: Are these pixels in this parametrisation equally distributed? Because we are examining a spiral of which we want to use the limiting behaviour, the answer to this question is yes, but only in the limit, which we can see in figure (5). We use three different number of turns and equally spaced pixels on the spiral (proportional to a factor, the spaces between N_i and N_j are different, the result would not change but the deviation would not be that figuratively). The first histogram shows us that for a high number of turns (marked blue) we get equally distributed pixels along the $\cos\theta$, which runs from -1 to 1 for a constant φ which we choose randomly. The second histogram shows us the distribution along the θ-angle, which runs from $[0, \pi]$. We can clearly see that near the equator are more pixels to count than at the poles, which is due to the periodicity of the spiral around the sphere. One angle is left: The φ-angle. We counted all pixels sorted those by their φ-angle, these pixels are equally distributed for all three Ns. But if we choose the number of turns N well below 100, the deviation would be clearly visible.

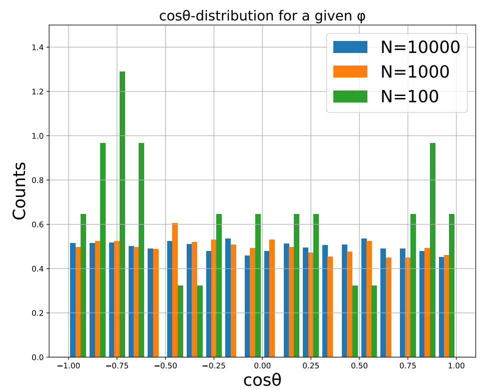

Figure 5: Distribution of pixels at $\cos\theta$

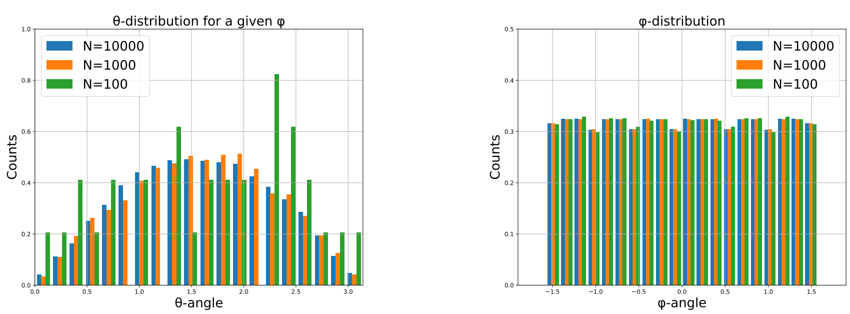

(a) θ-distribution

(b) φ-distribution

Figure 6: (θ, φ) - distribution counts for different number of turns.

2.2 Tangent plane

From there we can easily calculate the tangent vector of the spiral and because the curve depends only on the starting and endpoint we can postulate a second vector which will always be orthogonal to the tangent vector $\vec{t}$ and tangent to the surface of the sphere, those two vectors will in fact span our tangent plane.

The tangent vector is derived by the derivative along the curve:

$$t^i = \frac{\partial \gamma^i}{\partial \theta} \text{ or we could also } t^i = \frac{\partial \gamma^i}{\partial B} \tag{2.4}$$

with $i \in \{1, 2, 3\}$ denoting one of the components of $\vec{\gamma}$. Normalized with

$$\mathcal{N} = \frac{1}{\sqrt{1 + 4N^2(\frac{2B}{\sqrt{1+4N^2}} - \frac{B^2}{1+4N^2})}}$$

$$\begin{aligned}
t^1 &= \mathcal{N}\Big[\Big(1 - \frac{B}{1 + 4N^2}\Big) \cos\Big(2N \arccos(1 - \frac{B}{1 + 4N^2})\Big) \\
&\quad - 2N \sqrt{\frac{2B}{\sqrt{1 + 4N^2}} - \frac{B^2}{1 + 4N^2}} \sin\Big(2N \arccos(1 - \frac{B}{1 + 4N^2})\Big)\Big] \\
t^2 &= \mathcal{N}\Big[\Big(1 - \frac{B}{1 + 4N^2}\Big) \sin\Big(2N \arccos(1 - \frac{B}{1 + 4N^2})\Big) \\
&\quad + 2N \sqrt{\frac{2B}{\sqrt{1 + 4N^2}} - \frac{B^2}{1 + 4N^2}} \cos\Big(2N \arccos(1 - \frac{B}{1 + 4N^2})\Big)\Big] \\
t^3 &= -\mathcal{N} \sqrt{\frac{2B}{\sqrt{1 + 4N^2}} - \frac{B^2}{1 + 4N^2}}
\end{aligned} \tag{2.5}$$

This tangent vector can be described by the unit vectors $\vec{e}_\theta, \vec{e}_\varphi$ of the sphere, which is a natural orthogonal system in the (θ, φ)-basis. Our tangent vector looks decomposed like that:

$$\vec{t} = \frac{1}{\sqrt{1 + M^2}} \begin{bmatrix} 1 \\ M \end{bmatrix}_{(\theta,\varphi)} \tag{2.6}$$

while $M = 2N \cdot \sqrt{\frac{2B}{\sqrt{1+4N^2}} - \frac{B^2}{1+4N^2}}$. We want to discuss very shortly the properties of the function $M(B)$, this function is positive and has no singularities in $\mathbb{R}$. The behaviour is plotted in figure (7) for $N = 100$, $N = 500$ and $N = 1000$.

(2.8) is our tangent vector $\vec{t}$, its orthogonal vector, expressed in the (θ, φ)-basis, tangential to the surface of the sphere is:

$$\vec{s} = \frac{1}{\sqrt{1 + M^2}} \begin{bmatrix} -M \\ 1 \end{bmatrix}_{(\theta,\varphi)} \tag{2.7}$$

We can easily prove that they are orthonormal:

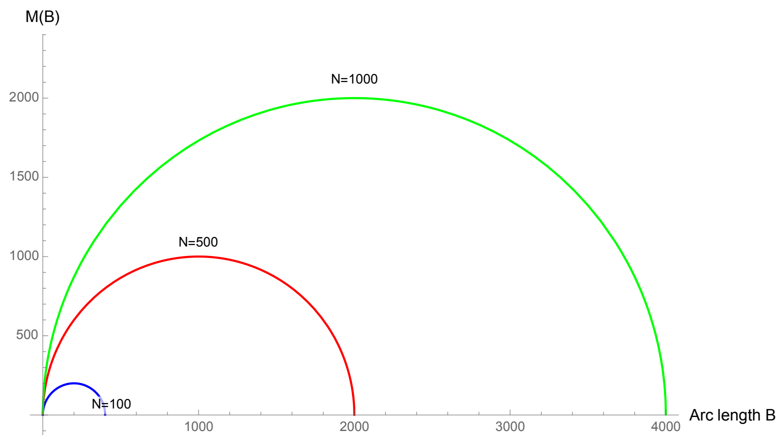

Figure 7: function M depending on number of turns and the arc length

$$
\begin{aligned}
\vec{t}\cdot\vec{s} &= \frac{1}{1+M^2}\Big[1\cdot(-M)+M\cdot 1\Big] \\
&= 0 \\
\vec{t}\cdot\vec{t} &= \frac{1}{1+M^2}\Big[1+M^2\Big] \\
&= 1 \\
\vec{s}\cdot\vec{s} &= \frac{1}{1+M^2}\Big[M^2+1\Big] \\
&= 1
\end{aligned}
\tag{2.8}
$$

Renaming the vectors (t, s) into (u, v) and placing them into a more differential geometric expression delivers:

$$
\partial_u = \frac{1}{\sqrt{1+M^2}}\cdot(\partial_\theta + M\partial_\varphi),\quad \partial_v = \frac{1}{\sqrt{1+M^2}}\cdot(\partial_\varphi - M\partial_\theta) \tag{2.9}
$$

This is our orthonormal system along the path of our spiral on the S^2.

2.3 Angle between $(\vec{t}, \vec{e}_\varphi)$ and $(\vec{t}, \vec{e}_\theta)$

We are interested in the difference between the tangent vector of the curve and the two unit vectors of the sphere. We expect that the angle between the tangent vector $\vec{t}$ and the φ-vector $\vec{e}_\varphi$ are the same for the equator, because we have already seen that the spiral is parallel to the latitude circles for large N. At the poles it is not possible to determine an angle, because the $\vec{e}_\varphi$ vector has at this region no preferred direction, but for our spiral we have a specific angle once we set up the spiral. So we can say, that we expect a dependency on the number of turns of the spiral and of course a dependency on the arc length.

2.3.1 Angle between $(\vec{t}, \vec{e}_\varphi)$

We use the tangent vector determined in (2.8) and the following unit vector:

$$\vec{e}_\varphi = \begin{bmatrix} -\sin(2N\theta) \\ \cos(2N\theta) \\ 0 \end{bmatrix} \tag{2.10}$$

Lets calculate the angle:

$$\begin{aligned} \vec{t}\cdot\vec{e}_\varphi &= \frac{1}{\sqrt{1+M^2}}\Big[-(1-\frac{B}{\sqrt{1+4N^2}})\cos(2N\theta)\sin(2N\theta) + M\sin(2N\theta)\sin(2N\theta) \\ &+ (1-\frac{B}{\sqrt{1+4N^2}})\sin(2N\theta)\cos(2N\theta) + M\cos(2N\theta)\cos(2N\theta)\Big] \\ &= \frac{M}{\sqrt{1+M^2}}\Big[\sin^2(2N\theta)+\cos^2(2N\theta)\Big] \\ &= \frac{M}{\sqrt{1+M^2}} \end{aligned} \tag{2.11}$$

which is expressed through the arc length and the number of turns:

$$\vec{t}\cdot\vec{e}_\varphi = \Big[\frac{1}{1+\frac{(1+4N^2)}{4N^2(2\sqrt{1+4N^2}-B)B}}\Big]^{1/2} \tag{2.12}$$

we can plot this and have a look at a special case of $N = 100$ which tells us the upper bound of the arc length $B = 2\cdot\sqrt{1+4N^2} \cong 400$ (Just in case of curiosity the error is about 0.00124%) also we calculated the real-valued limiting behaviour of the scalar product:

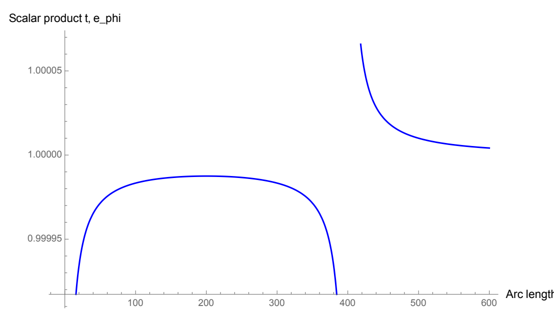

Figure 8: Scalar product of $\vec{t}$ and $\vec{e}_\varphi$ along the arc length B.

$$\begin{aligned} \lim_{B\to 2\sqrt{1+4N^2}}\Big[\frac{1}{1+\frac{(1+4N^2)}{4N^2(2\sqrt{1+4N^2}-B)B}}\Big]^{1/2} &= 0 \\ \lim_{B\to 0}\Big[\frac{1}{1+\frac{(1+4N^2)}{4N^2(2\sqrt{1+4N^2}-B)B}}\Big]^{1/2} &= 0 \end{aligned} \tag{2.13}$$

We can see from the limit that the two vectors are always orthogonal at the poles, due to the non defined direction of the $\vec{e}_\varphi$ unit vector and nearly parallel at the equator.

2.3.2 Angle between $(\vec{t}, \vec{e}_\theta)$

The $\vec{e}_\theta$ unit vector tells us the direction on the longitudes (while the angle θ tells us on which latitude we are.), what we expect is of course that at the equator the tangent vector and the $\vec{e}_\theta$-unit vector are orthogonal, and therefore the scalar product would vanish. Vice versa, we expect the scalar product to be 1 at the poles, because for a chosen spiral, we have a well-defined direction of the tangent vector and the $\vec{e}_\theta$ is also well-defined, therefore this should hold for the scalar product. With the $\vec{e}_\theta$-unit vector we can start calculating the scalar product.

$$\vec{e}_\theta = \begin{bmatrix} \cos\theta\, \cos(2N\theta) \\ \cos\theta\, \sin(2N\theta) \\ -\sin\theta \end{bmatrix} \tag{2.14}$$

Lets calculate the angle again:

$$\begin{aligned} \vec{t}\cdot\vec{e}_\theta = \frac{1}{\sqrt{1+M^2}}\Big[&(1-\frac{B}{\sqrt{1+4N^2}})\, \cos(2N\theta)\, \cos\theta\, \cos(2N\theta) \\ &+ (1-\frac{B}{\sqrt{1+4N^2}})\sin(2N\theta)\, \cos\theta\, \sin(2N\theta) \\ &- M\sin(2N\theta)\, \cos(\theta)\, \cos(2N\theta) \\ &+ M\cos(2N\theta)\, \cos(\theta)\, \sin(2N\theta) \\ &+ \frac{M}{2N}\, \sin\theta\Big] \\ = \frac{1}{\sqrt{1+M^2}}\Big[&(1-\frac{B}{\sqrt{1+4N^2}})\cos\theta(\sin^2(2N\theta)+\cos^2(2N\theta)) + \frac{M}{2N}\sin\theta\Big] \\ = \frac{1}{\sqrt{1+M^2}}\Big[&(1-\frac{B}{\sqrt{1+4N^2}})\, \cos\theta + \frac{M}{2N}\sin\theta\Big] \end{aligned} \tag{2.15}$$

uthe relation $\cos\theta = 1 - \frac{B}{\sqrt{1+4N^2}}$ and deriving the following:

$$\begin{aligned} \cos\theta &= 1 - \frac{B}{\sqrt{1+4N^2}} \\ \cos^2\theta &= 1 - \frac{2B}{\sqrt{1+4N^2}} + \frac{B^2}{1+4N^2} \\ 1-\sin^2\theta &= 1 - \frac{2B}{\sqrt{1+4N^2}} + \frac{B^2}{1+4N^2} \\ \sin\theta &= \sqrt{\frac{2B}{\sqrt{1+4N^2}} - \frac{B^2}{1+4N^2}} \\ \sin\theta &= \frac{M}{2N} \end{aligned} \tag{2.16}$$

we end up at:

$$
\begin{aligned}
\vec{t}\cdot\vec{e}_\theta &= \frac{1}{\sqrt{1+M^2}}\Big[(1-\frac{B}{\sqrt{1+4N^2}})\,\cos\theta+\frac{M}{2N}\sin\theta\Big]\\
&= \frac{1}{\sqrt{1+M^2}}\Big[(1-\frac{B}{\sqrt{1+4N^2}})^2+(\frac{M}{2N})^2\Big]\\
&= \frac{1}{\sqrt{1+M^2}}\Big[1-\frac{2B}{\sqrt{1+4N^2}}+\frac{B^2}{1+4N^2}+\frac{2B}{\sqrt{1+4N^2}}-\frac{B^2}{1+4N^2}\Big]\\
&= \frac{1}{\sqrt{1+M^2}}
\end{aligned}
\tag{2.17}
$$

Expressed only through the arc length and the number of turns:

$$
\vec{t}\cdot\vec{e}_\theta = \frac{1}{\sqrt{1+4N^2(\frac{2B}{\sqrt{1+4N^2}}-\frac{B^2}{1+4N^2})}}
\tag{2.18}
$$

We can already see, that this scalar product does not diverge for real values $N, B \in \mathbb{R}$ also we can see that for $B = 0$ the angle between $\vec{t}$ and $\vec{e}_\theta$ is 1, which means they are parallel, vice versa orthogonal at the equator: For $B = \sqrt{1+4N^2} \cong 200$ we get $\vec{t}\cdot\vec{e}_\theta = 0$, which is the orthogonal relation.

$$
\begin{aligned}
\lim_{B\to 2\sqrt{1+4N^2}}\Big[\frac{1}{\sqrt{1+4N^2(\frac{2B}{\sqrt{1+4N^2}}-\frac{B^2}{1+4N^2})}}\Big] &= 1\\
\lim_{B\to 0}\Big[\frac{1}{\sqrt{1+4N^2(\frac{2B}{\sqrt{1+4N^2}}-\frac{B^2}{1+4N^2})}}\Big] &= 1
\end{aligned}
\tag{2.19}
$$

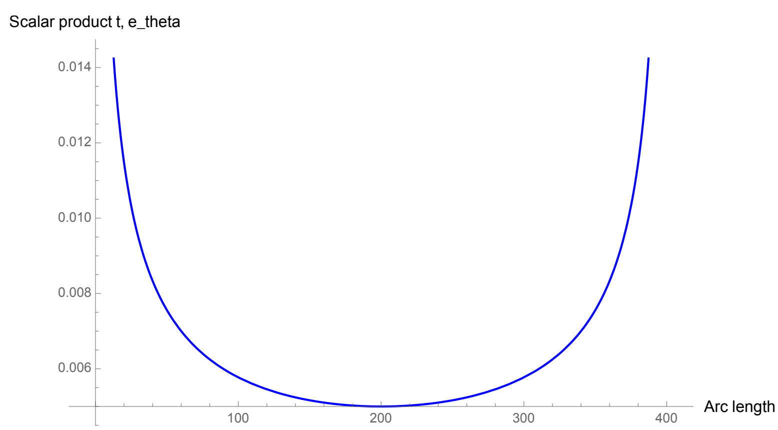

Figure 9: Scalar product of $\vec{t}$ and $\vec{e}_\theta$ along the arc length B.

3 Differential geometric aspects

3.1 Is the curve a geodesic?

A geodesic is a curve which connects two points along the shortest path between them. The definition does not hold for our curve, basic example would be two points with different θ-angles but same φ-angle, those points would be beneath each other. The curve would have to make hole loops to connect one point with the other one, while these loops do not match great circles, the curve as a whole can not be a geodesic. Nevertheless to show this thesis, we would like to calculate the geodesic equation for our curve, which is realised by:

$$\frac{\mathrm{d}\gamma^k}{\mathrm{d}B} + \Gamma^k_{ij}\frac{\mathrm{d}\gamma^i}{\mathrm{d}B}\frac{\mathrm{d}\gamma^i}{\mathrm{d}B} = 0 \tag{3.1}$$

With B being the arc length of the curve, $\vec{\gamma}$ the parametrisation of the curve in the (θ, φ)-basis from equation (1.1) and indices $k, i, j \in \{1, 2\}$. In this basis we know all the Christoffel symbols:

$$\Gamma^{\varphi}_{\varphi\theta} = \Gamma^{\varphi}_{\theta\varphi} = \cot(\theta) = \frac{1 - \frac{B}{\sqrt{1+4N^2}}}{\sqrt{1 - (1 - \frac{B}{\sqrt{1+4N^2}})^2}} \tag{3.2}$$

and

$$\Gamma^{\theta}_{\varphi\varphi} = -\sin(\theta)\cos(\theta) = \left(1 - \frac{B}{\sqrt{1+4N^2}}\right)\sqrt{1 - (1 - \frac{B}{\sqrt{1+4N^2}})^2} \tag{3.3}$$

while we used for the substitution equation (1.1). Now we still need to express the parametrisation through the arc length:

$$\vec{\gamma} = \left(\arccos(1 - \frac{B}{\sqrt{1+4N^2}}), 2N\arccos(1 - \frac{B}{\sqrt{1+4N^2}})\right)^{\perp}_{(\theta,\varphi)} \tag{3.4}$$

From here we can calculate the entries in the geodesic equation, because our curve only depends on the θ-angle the only derivatives we need to derive are $\frac{\mathrm{d}\theta}{\mathrm{d}B}$ and $\frac{\mathrm{d}^2\theta}{\mathrm{d}B^2}$:

$$\frac{\mathrm{d}\theta}{\mathrm{d}B} = \frac{1}{\sqrt{1+4N^2}\sqrt{1 - (1 - \frac{B}{\sqrt{1+4N^2}})}} \tag{3.5}$$

$$\frac{\mathrm{d}^2\theta}{\mathrm{d}B^2} = -\frac{1 - \frac{B}{\sqrt{1+4N^2}}}{(1+4N^2)(1 - (1 - \frac{B}{\sqrt{1+4N^2}})^2)^{3/2}} \tag{3.6}$$

Now, we can plug them into our geodesic equation, for the first component we get:

$$\begin{aligned} 0 &\overset{!}{=} \frac{\mathrm{d}^2\theta}{\mathrm{d}B^2} + \Gamma^{\theta}_{\varphi\varphi}\frac{\mathrm{d}\varphi}{\mathrm{d}B}\frac{\mathrm{d}\varphi}{\mathrm{d}B} \\ &= -\frac{1 - \frac{B}{\sqrt{1+4N^2}}}{1+4N^2}\Big(\frac{1}{(1 - (1 - \frac{B}{\sqrt{1+4N^2}})^2)^{3/2}} + 4N^2\sqrt{1+4N^2}\Big) \end{aligned} \tag{3.7}$$

So the first geodesic equation only vanishes if $B = \sqrt{1+4N^2}$, this is the equatorial plane on the sphere, because we calculated from equation (2.2), that the arc length walks from 0 to $2\sqrt{1+4N^2}$. This means that we can find a geodesic at $\theta = \pi/2$, which seems reasonable, because the curve at the equator is nearly parallel to a great circle, it is important that this only holds for $N \gg 1$, this was used in the derivation of the arc length, that means that there would not exist a geodesic at the equator for our curve for example with $N = 10$.

Lets calculate the geodesic equation for the second component!

$$\begin{aligned}
0 &\stackrel{!}{=} \frac{\mathrm{d}^2\varphi}{\mathrm{d}B^2} + \Gamma^{\varphi}_{\varphi\theta}\frac{\mathrm{d}\varphi}{\mathrm{d}B}\frac{\mathrm{d}\theta}{\mathrm{d}B} + \Gamma^{\varphi}_{\theta\varphi}\frac{\mathrm{d}\theta}{\mathrm{d}B}\frac{\mathrm{d}\varphi}{\mathrm{d}B} \\
&= \frac{\mathrm{d}^2\varphi}{\mathrm{d}B^2} + 2\Gamma^{\varphi}_{\varphi\theta}\frac{\mathrm{d}\varphi}{\mathrm{d}B}\frac{\mathrm{d}\theta}{\mathrm{d}B} \\
&= -N\frac{1-\frac{B}{\sqrt{1+4N^2}}}{(1+4N^2)(1-(1-\frac{B}{\sqrt{1+4N^2}})^2)^{3/2}}
\end{aligned} \tag{3.8}$$

Also this geodesic equation vanishes for $B = \sqrt{1+4N^2}$.

3.2 Metric

We want to look deeper into the geometric aspects of the spiral, therefore we can calculate the metric from the chosen coordinates. As reminder the coordinates along the spiral are given by:

$$\begin{aligned}
\partial_u &= \frac{1}{\sqrt{1+M^2}}(\partial_\theta + M\partial_\varphi) \\
\partial_v &= \frac{1}{\sqrt{1+M^2}}(\partial_\varphi - M\partial_\theta)
\end{aligned} \tag{3.9}$$

With $M := M(B,N) = 2N\sqrt{\frac{2B}{\sqrt{1+4N^2}} - (\frac{B}{\sqrt{1+4N^2}})^2}$, B still being the arc length and N the number of turns of the spiral around the sphere. For this function we find $M(B) \geq 0$ in the range $B \in [0, 2\sqrt{1+4N^2}]$. Geodesics on the sphere are calculated through the scalar product $\mathrm{d}s^2 = g_{ab}\mathrm{d}x^a\mathrm{d}x^b$, which is described through the metric, in the matrix representation (which I denote here as $(h_{\mu\nu})$ for h being a metric) it looks like that in the (θ, φ) basis:

$$(g_{ab}) = \begin{pmatrix} 1 & 0 \\ 0 & \sin^2\theta \end{pmatrix} \tag{3.10}$$

And from there it is an easy way to compute our metric, represented through ∂_u and ∂_v. Through the relationship

$$g'_{ab} = \frac{\partial x^c}{\partial x^a}\frac{\partial x^d}{\partial x^b}g_{cd} \tag{3.11}$$

we get

$$(g_{ab}) = \frac{1}{1+M^2}\begin{pmatrix} 1+M^2\cdot\sin^2[\frac{1}{1+M^2}(u-Mv)] & -M\cdot\cos^2[\frac{1}{1+M^2}(u-Mv)] \\ \\ -M\cdot\cos^2[\frac{1}{1+M^2}(u-Mv)] & M^2+\sin^2[\frac{1}{1+M^2}(u-Mv)] \end{pmatrix} \quad (3.12)$$

And its inverse form with $\mathcal{N} = \frac{1}{\sin^2\theta(u,v)(1+M^2)}$:

$$(g^{ab}) = \mathcal{N}\begin{pmatrix} M^2+\sin^2[\frac{1}{1+M^2}(u-Mv)] & M\cos^2[\frac{1}{1+M^2}(u-Mv)] \\ \\ M\cos^2[\frac{1}{1+M^2}(u-Mv)] & 1+M^2\sin^2[\frac{1}{1+M^2}(u-Mv)] \end{pmatrix} \quad (3.13)$$

Which fullfils the relation $g_{ac}g^{cb} = \delta^b_a$.

3.3 Riemann tensor for a maximally symmetric manifold

From here on we can compute multiple quantities: Riemann-curvature, Ricci-tensor and of course to check our continuity the Ricci-scalar, which we know is $R = 2$ for a sphere. As we know, the sphere is a highly symmetric manifold and it is therefore very easy to calculate the Riemann-curvature:

$$R_{abcd} = \frac{R}{2}(g_{ac}g_{bd} - g_{ad}g_{bc}) \quad (3.14)$$

Important note: This formula has a more general form, but we simplified it by using the fact, that we are operating on the surface of a sphere, which is a 2-dimensional problem. This formula results from the Lie-derivative, the calculation is lengthy, but I would like to summarise the main steps.

We start by mentioning the Lie derivative

$$(\mathscr{L}_K g)_{\mu\nu} = \nabla_\nu K_\mu + \nabla_\mu K_\nu = 0 \quad (3.15)$$

for K being a Killing vector and g being the metric. Also the covariant derivatives do not commute which leads to

$$\Big[\nabla_c, \nabla_b\Big]\nabla_d K_e = \nabla_c R^a{}_{bde}K_a + R^f{}_{bde}\nabla_c K_f - \nabla R^a{}_{cde}K_a - R^f{}_{cde}\nabla_b K_f \quad (3.16)$$

But it is also possible to derive a different expression for the same equation:

$$\Big[\nabla_c, \nabla_b\Big]\nabla_d K_e = R^a{}_{dbc}\nabla_a K_e + R^a{}_{ebc}\nabla_d K_a \quad (3.17)$$

Setting those two different expressions we can end up with:

$$\Big[\nabla_c R^a{}_{bde} - \nabla_b R^a{}_{cde}\Big]K_a + \Big[R^f{}_{bde}\delta^a_c - R^f{}_{cde}\delta^a_b + R^a{}_{ebc}\delta^f_d - R^a{}_{dbc}\delta^f_e\Big]\nabla_a K_f = 0 \quad (3.18)$$

Which means the brackets must be zero, when we examine the second bracket and multiply δ^c_a we get:

$$R_{ad} = \frac{1}{n}g_{ad}R \quad (3.19)$$

with R being the Ricci-scalar. In the same calculation and using the above result one finds that

$$\begin{aligned}(n-1)R_{baed} &= -g_{ae}R_{db} + g_{ad}R_{eb}\\ R_{baed} &= \frac{R}{n(n-1)}\Big(g_{be}g_{ad} - g_{ae}g_{bd}\Big)\end{aligned} \tag{3.20}$$

R is the Ricci-scalar which we verified as $R = 2$ and we are working on a two dimensional problem, which returns a disappearing pre-factor, that gets us the Riemann-curvature: With formula (3.20) and the symmetries of the Riemann tensor we derive that there are only eight entries:

$$\begin{aligned}R_{uvvu} &= g_{uv}g_{vu} - g_{uu}g_{vv}\\ &= \frac{1}{(1+M^2)^2}\Big[(-M\cos^2\theta(u,v))^2 - (1+M^2\sin^2\theta(u,v))(M^2+\sin^2\theta(u,v))\Big]\\ &= \frac{1}{(1+M^2)^2}\Big[M^2(1-\sin^2\theta(u,v))^2 - M^2 - \sin^2\theta(u,v) - M^4\sin^2\theta(u,v) - M^2\sin^4\theta(u,v)\Big]\\ &= \frac{1}{(1+M^2)^2}\Big[-2M^2\sin^2\theta(u,v) + M^2\sin^4\theta(u,v) - \sin^2\theta(u,v) - M^4\sin^2\theta(u,v) - M^2\sin^4\theta(u,v)\Big]\\ &= \frac{1}{(1+M^2)^2}\Big[-(1+2M^2+M^4)\sin^2\theta(u,v)\Big]\\ &= \frac{1}{1+M^2}\Big[\Big(1+M^2\Big)^2(-\sin^2\theta(u,v))\Big]\\ &= -\sin^2\theta(u,v)\\ &= R_{vuuv} = -R_{uvuv} = -R_{vuvu} = -\sin^2(\theta(u,v))\end{aligned} \tag{3.21}$$

with $\theta(u,v) = \frac{1}{1+M^2}(u - Mv)$. From our previous observations we figured out that $M(B) \geq 0 \Rightarrow \frac{1}{1+M^2} \geq 0$ and also $\sin^2\theta(u,v) \geq 0$ from here we can conclude that all our Riemann tensor entries for any given number of turns anywhere on the spiral are negative.

3.4 Ricci-tensor and Ricci-scalar

The Ricci-tensor is then

$$R_{bd} = g^{ac} R_{abcd} \tag{3.22}$$

and with the computed Riemann-tensors and the symmetry of the Ricci-tensor we derive:

$$\begin{aligned}
R_{uu} &= \frac{[1 + M^2 \sin^2 \theta(u, v)] \sin^2 \theta(u, v)}{\sin^2 \theta(u, v)(1 + M^2)} \\
&= -\frac{1 + M^2 \sin^2 \theta(u, v)}{(1 + M^2)} \\
R_{vv} &= \frac{[M^2 + \sin^2 \theta(u, v)] \sin^2(\theta(u, v))}{\sin^2 \theta(u, v)(1 + M^2)} \\
&= \frac{M^2 + \sin^2 \theta(u, v)}{(1 + M^2)} \\
R_{uv} &= R_{vu} \\
&= -\frac{-M \cos^2 \theta(u, v) \sin^2 \theta(u, v)}{\sin^2 \theta(u, v)(1 + M^2)} \\
&= -\frac{M \cos^2 \theta(u, v)}{(1 + M^2)}
\end{aligned} \tag{3.23}$$

Just for fun, one can now compute the Ricci-scalar again (refer to appendix A.2),

$$\begin{aligned}
R &= g^{bd} R_{bd} \\
R &= g^{uu} R_{uu} + 2g^{uv} R_{uv} + g^{vv} R_{vv} \\
&= 2
\end{aligned} \tag{3.24}$$

4 Spherical harmonics

4.1 Δ and $\eth$ in the (u, v)-basis

The $\eth$ is defined in the (θ, φ)-basis and acts on a function η as followed:

$$\eth\,\eta = -(\sin\theta)^s \left(\partial_\theta + \mathrm{i}\csc\theta\partial_\varphi\right)(\sin\theta)^{-s}\eta \tag{4.1}$$

$$\bar{\eth}\eta = -(\sin\theta)^s \left(\partial_\theta - \mathrm{i}\csc\theta\partial_\varphi\right)(\sin\theta)^{-s}\eta \tag{4.2}$$

By substituting (3.9) we get:

$$\eth\,\eta = -\Big(\frac{M}{2N}\Big)^s\Big[\frac{1}{\sqrt{1+M^2}}\Big((\partial_u - M\partial_v) + \mathrm{i}\frac{2N}{M}(\partial_v + M\partial_u)\Big)\Big]\Big(\frac{M}{2N}\Big)^{-s}\eta \tag{4.3}$$

$$\bar{\eth}\eta = -\Big(\frac{M}{2N}\Big)^s\Big[\frac{1}{\sqrt{1+M^2}}\Big((\partial_u - M\partial_v) - \mathrm{i}\frac{2N}{M}(\partial_v + M\partial_u)\Big)\Big]\Big(\frac{M}{2N}\Big)^{-s}\eta \tag{4.4}$$

This means we can interchange spin-weighted spherical harmonics on a tangent plane on our spiral from the (θ, φ)-basis to the (u, v)-basis. Nevertheless, we would like to get real, by the relation between the edth-operator and the Laplace operator:

$$\Delta = \frac{1}{2}\cdot[\eth\,\bar{\eth} + \bar{\eth}\,\eth] \tag{4.5}$$

$$\Delta_{u,v} = \frac{1}{1+M^2}\Big[\Big(1+4N^2\Big)\partial_u^2 + 2M\Big(\frac{4N^2}{M^2} - 1\Big)\partial_u\partial_v + \Big(M^2 + \frac{4N^2}{M^2}\Big)\partial_v^2\Big] \tag{4.6}$$

This fulfills our triangle, we can now interchange between the three differentials: $\Delta_{\theta,\varphi}$, $\Delta_{u,v}$ and $\eth$.

4.2 Solution to the eigenvalue problem

By deriving the Laplacian in the (u, v)-basis it is now time to postulate the solution to the Laplacian equation in the (u, v)-coordinates. The Laplace-equation is a linear differential equation and it is natural that the solution in our (u, v)-basis is a linear combination of the spherical harmonics, an easy example is a wave which travels from one point at the equator to the opposite site of the sphere along the spiral. This wave would cross multiple forms of the spherical harmonics and therefore different (ℓ, m)-combinations. So this wave would be a linear combination of these $Y_{\ell m}$-combinations. From this we start by writing the Laplace equation in our (u, v)-basis:

$$\Delta_{u,v}\tilde{Y}_{\ell m}(u, v) = -\ell(\ell+1)\tilde{Y}_{\ell m}(u, v) \tag{4.7}$$

The linear combination is expressed like:

$$\tilde{Y}_{\ell m}(u, v) = \sum_{i=0}^{\ell}\sum_{n=-m}^{m} A_{(i,n)}Y_{in}(u, v) \tag{4.8}$$

while the spherical harmonics in the (u, v)-basis are expressed as:

$$Y_{\ell m}(u,v) = \sqrt{\frac{2\ell+1}{4\pi}\frac{(\ell-m)!}{(\ell+m)!}} P_\ell^m\Big[\cos\Big(\frac{1}{\sqrt{1+M^2}}(u-Mv)\Big)\Big]\exp\Big[\frac{2imN}{\sqrt{1+M^2}}(u-Mv)\Big] \tag{4.9}$$

Due to the orthonormality of the spherical harmonics the coefficients $A_{(\ell,m)}$ can be derived by the scalar product.

$$\begin{aligned} A_{(r,s)} &= \langle Y_{rs}, \tilde{Y}_{\ell m}\rangle \\ &= \int_{S^2} Y_{rs}^* \, \tilde{Y}_{\ell m} \, \mathrm{d}\Omega \\ &= \int_{S^2} Y_{rs}^* \sum_{i=0}^{\ell}\sum_{n=-m}^{m} A_{(i,n)} Y_{in} \, \mathrm{d}\Omega \\ &= \int_{S^2} \sum_{i=0}^{\ell}\sum_{n=-m}^{m} A_{(i,n)} Y_{rs}^* Y_{in} \, \mathrm{d}\Omega \\ &= \sum_{i=0}^{\ell}\sum_{n=-m}^{m} A_{(i,n)} \int_{S^2} Y_{rs}^* Y_{in} \, \mathrm{d}\Omega \\ &= \sum_{i=0}^{\ell}\sum_{n=-m}^{m} A_{(i,n)} \delta_{ri}\delta_{sn} \\ &= A_{(r,s)} \end{aligned} \tag{4.10}$$

It is worth mentioning that the coefficient A_{rs} accounts for the spherical harmonic Y_{rs}, $\tilde{Y}_{\ell m}$ is than spanned through a linear combination of those coefficients and spherical harmonics.

Because our Laplacian is a product of plane Cartesian coordinates, we can directly evaluate an obvious solution to the Eigenvalue problem:

$$\Delta_{u,v}\tilde{y}(u,v) = -\tilde{y}(u,v) \text{ with } \tilde{y}(u,v) = \exp\Big(i\frac{u-Mv}{\sqrt{1+M^2}}\Big) \tag{4.11}$$

$$
\begin{aligned}
\Delta_{u,v}\tilde{y}(u,v) &= \frac{1}{1+M^2}\Big[(1+4N^2)\partial_u^2 + 2M(\frac{4N^2}{M^2}-1)\partial_u\partial_v + (M^2+\frac{4N^2}{M^2})\partial_v^2\Big]\exp\Big(i\frac{u-Mv}{\sqrt{1+M^2}}\Big)\\
&= \frac{i^2}{(1+M^2)^2}\Big[(1+4N^2) + 2M(\frac{4N^2}{M^2}-1)(-M) + (M^2+\frac{4N^2}{M^2})M^2\Big]\exp\Big(i\frac{u-Mv}{\sqrt{1+M^2}}\Big)\\
&= \frac{i^2}{(1+M^2)^2}\Big[1+4N^2-8N^2+2M^2-M^4+4N^2\Big]\exp\Big(i\frac{u-Mv}{\sqrt{1+M^2}}\Big)\\
&= \frac{-1}{(1+M^2)^2}\Big[1+2M^2+M^4\Big]\exp\Big(i\frac{u-Mv}{\sqrt{1+M^2}}\Big)\\
&= -\frac{(1+M^2)^2}{(1+M^2)^2}\exp\Big(i\frac{u-Mv}{\sqrt{1+M^2}}\Big)\\
&= -\exp\Big(i\frac{u-Mv}{\sqrt{1+M^2}}\Big)
\end{aligned}
\tag{4.12}
$$

This means that plane waves are solving our Laplace equation in the tangent plane along the spiral.

5 Summary

The idea behind this thesis is to map pixels on the surface of a sphere onto a flat plane. We are observing waves on the sphere and decompose them through spherical harmonics, this decomposition can be represented through Fourier transformations on a flat plane, therefore we are operating in tangent spaces.

Pixelisation: The Igloo pixelisation [2] is for a spiral an appropriate candidate. The number of turns which is determined through the resolution of the data, would determine the height of the pixels so that every pixel would only cross each pixel once. This is important to eliminate any recurring data along the spiral, which would not be present.

Geometry: A path is nice to handle because it is only one parameter B, the arc length, necessary to describe a position $\vec{x}$ on the surface of a sphere. With this we derived two unit vectors $\vec{t}$ and $\vec{s}$, which span a tangent plane on the surface of the sphere along the spiral. For the Archimedean spiral with a high number of turns, the tangent vector and the unit vector $\vec{e}_\varphi$ become parallel, except near and at the poles, where $\vec{e}_\varphi$ loses importance. The vector $\vec{t}$ is orthogonal to the θ-unit vector $\vec{e}_\theta$ of the sphere, except near the poles/at the poles, simple because the tangent vector starts at the pole, a dot, and needs to get into a circular motion.

This enables us to calculate the Riemann metric $g_{\mu\nu}$, which describes the geometry on this manifold. A parameter which informs us about the curvature of a manifold is the Ricci scalar R, which happens to be 2 for the surface of the sphere, we verified the legitimacy of our new tangent plane coordinates by calculating R. By deriving the Ricci scalar we found out that all entries of the Riemann tensor R_{abcd} are negative.

Further we asked when does our curve become a geodesic. Which is on the sphere equivalent to asking when does the curve become a great circle, which is more visible to answer: At the equator, but only for a high number of turns N.

Wave decomposition: Spherical waves are decomposed into spherical harmonics, which are eigenfunctions of the Laplace equation, the limit behavior of the Laplace equation generates plane waves, expressing the Laplace equation in a tangent plane basis ∂_u and ∂_v generates functions which are directly related to the spherical harmonics but are functions of the tangent plane. The decomposition of functions in a plane is carried out with Fourier transformations, therefore it is reasonable that a plane wave solves the Laplace equation. Unfortunately I was not able to derive a recursion relation for the coefficients of the eigenfunction of the Laplace equation expressed in the (u, v)-basis.

References

[1] Martin Duhamel Pierre ; Vetterli. "Fast Fourier transforms: A tutorial review and a state of the art". In: (1990). DOI: https://infoscience.epfl.ch/record/59946.

[2] Neil G. Turok Robert G. Crittenden. "Exactly Azimuthal Pixelizations of the Sky". In: (1998), p. 3. DOI: arXiv:astro-ph/9806374v1.

[3] Clive Temperton. "A generalized prime factor FFT algorithm for any $N = 2^p3^q5^r$". In: (1992). DOI: https://doi.org/10.1137/0913039.

[4] Eric Weisstein. "Great Circle". In: (). DOI: https://mathworld.wolfram.com/GreatCircle.html.

A Appendix

A.1 Arc length approximation

For the arc length derivation we get an incomplete elliptic integral of the second kind $E(\theta, 2Ni)$:

$$\begin{aligned} B &= \int_a^b \mathrm{d}\theta \sqrt{\dot{x^2} + \dot{y^2} + \dot{z^2}} \\ &= \int_0^\theta \mathrm{d}\theta' \sqrt{1 + 4N^2 \sin^2\theta'} \\ &= \int_0^\theta \mathrm{d}\theta' b(N, \theta') \end{aligned} \tag{A.1}$$

This is not analytical solvable and therefore we search for a approximated integrand. We already saw that for $\theta = \{0, \pi\}$ the integrand must be 1 and for $\theta = \pi/2$ the integrand must be $\sqrt{1 + 4N^2}$. These conditions are fulfilled by the function:

$$\tilde{b}(N, \theta) = \left(\sqrt{1 + 4N^2} - 1\right) \sin\theta + 1$$

Both integrals are plotted against the latitude angle θ for N = 100:

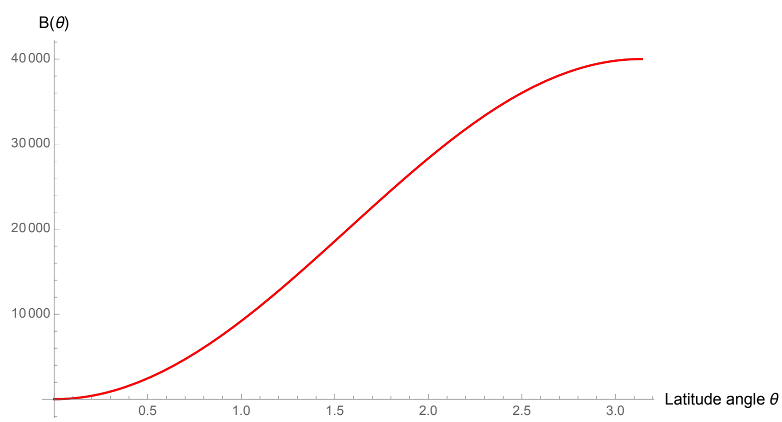

Figure 10: Integrated b and $\tilde{b}$, which lay beneath each other.

While the red line is the elliptic integral and the blue one (which is not even visible) is the approximated integral. The error of the upper approximation is displayed in the next plot (11). It is important to notice, that the function $\frac{b - \tilde{b}}{b}$ is not diverging for small angles θ.

The error minimizes by increasing N the number of turns.

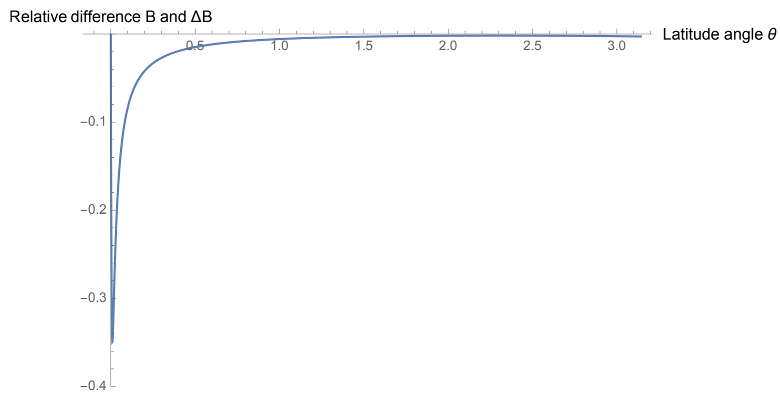

Figure 11: Relative difference between the integrated b and $\tilde{b}$.

A.2 Ricci scalar in (u, v)-basis.

The calculation of the Ricci scalar is a bit lengthy, I color-coded the canceling terms, the summarized terms and the substituted terms.

$$
\begin{aligned}
R &= g^{bd}R_{bd} \\
&= g^{uu}R_{uu} + 2g^{uv}R_{uv} + g^{vv}R_{vv} \\
&= \frac{M^2 + \sin^2\theta(u,v)}{\sin^2\theta(u,v)(1+M^2)}\frac{1 + M^2\sin^2\theta(u,v)}{1+M^2} + 2\frac{M\cos^2\theta(u,v)}{\sin^2\theta(u,v)(1+M^2)}\left(-\frac{M\cos^2\theta(u,v)}{1+M^2}\right) \\
&+ \frac{1 + M^2\sin^2\theta(u,v)}{\sin^2\theta(u,v)(1+M^2)}\frac{M^2 + \sin^2\theta(u,v)}{1+M^2} \\
&= \frac{1}{\sin^2\theta(u,v)(1+M^2)^2}\Big[(M^2 + \sin^2\theta(u,v))(1 + M^2\sin^2\theta(u,v)) - 2M^2\cos^4\theta(u,v) \\
&+ (1 + M^2\sin^2\theta(u,v))(M^2 + \sin^2\theta(u,v))\Big] \\
&= \frac{1}{\sin^2\theta(u,v)(1+M^2)^2}\Big[M^2 + M^4\sin^2\theta(u,v) + \sin^2\theta(u,v) + M^2\sin^4\theta(u,v) - 2M^2\cos^4\theta(u,v) \\
&+ M^2 + \sin^2\theta(u,v) + M^4\sin^2\theta(u,v) + M^2\sin^4\theta(u,v)\Big] \\
&= \frac{1}{\sin^2\theta(u,v)(1+M^2)^2}\Big[2M^2 + 2M^4\sin^2\theta(u,v) + 2\sin^2\theta(u,v) + 2M^2\sin^4\theta(u,v) \\
&- 2M^2(1 - 2\sin^2\theta(u,v) + \sin^4\theta(u,v))\Big] \\
&= \frac{1}{\sin^2\theta(u,v)(1+M^2)^2}\Big[2M^2 + 2M^4\sin^2\theta(u,v) + 2\sin^2\theta(u,v) + 2M^2\sin^4\theta(u,v) \\
&- 2M^2 + 4M^2\sin^2\theta(u,v) - 2M^2\sin^4\theta(u,v)\Big] \\
&= \frac{1}{\sin^2\theta(u,v)(1+M^2)^2}\Big[2M^4\sin^2\theta(u,v) + 2\sin^2\theta(u,v) + 4M^2\sin^2\theta(u,v)\Big] \\
&= \frac{\sin^2\theta(u,v)}{\sin^2\theta(u,v)(1+M^2)^2}\Big[2M^4 + 2 + 4M^2\Big] \\
&= 2\frac{1}{(1+M^2)^2}(1+M^2)^2 \\
&= 2
\end{aligned}
\tag{A.2}
$$

B Erklärung

Ich versichere, dass ich diese Arbeit selbstständig verfasst und keine anderen als die angegebenen Quellen und Hilfsmittel benutzt habe.

Heidelberg, den 13.08.2020,